



## Monitor the freshness of shrimp by smart halochromic films based on gelatin/pectin loaded with pistachio peel anthocyanin nanoemulsion

Alireza Taheri-Yeganeh<sup>a</sup>, Hamed Ahari<sup>a,\*</sup>, Zohreh Mashak<sup>b</sup>, Seid Mahdi Jafari<sup>c</sup>

<sup>a</sup> Department of Food Science and Technology, Science and Research Branch, Islamic Azad University, Tehran, Iran

<sup>b</sup> Department of Food Hygiene, Karaj Branch, Islamic Azad University, Karaj, Iran

<sup>c</sup> Department of Food Materials & Process Design Engineering, Gorgan University of Agricultural Sciences and Natural Resources, Gorgan, Iran

### ARTICLE INFO

#### Keywords:

Nanoemulsion  
Anthocyanins  
Intelligent packaging  
Sustainability  
Freshness monitoring

### ABSTRACT

This paper focuses on the combination of gelatin (Gel), pectin (Pec), and Pistachio peel anthocyanins (PSAs) to develop a halochromic film for food applications (shrimp). The results of spectroscopic properties showed that the film components had proper interaction and compatibility. Furthermore, the addition of PSAs and Pec improved the thermal stability of films. The addition of Pec and PSAs significantly improved the physical properties and mechanical resistance of the films. So that, the permeability to water vapor and oxygen reduced from 2.81 to 2.74 ( $\text{g}\cdot\text{s}^{-1}\cdot\text{Pa}^{-1}\cdot\text{m}^{-1}$ ) and 5.25 to 4.70 ( $\text{meq}/\text{kgO}_2$ ), respectively. In addition, the strength and flexibility of halochromic film reached 0.7 MPa and 56 % compared to Gel film (0.62 MPa, and 46.96 %). Most importantly, the color changes of the smart film from cherry/pink to yellow/brown, which were proportional to the color changes of the anthocyanin solution at different pHs, were able to monitor the shrimp freshness and spoilage at room (20 °C) and refrigerated (4 °C) temperature for 14 days.

### Introduction

Packaging plays a crucial role in preserving the quality and extending the shelf life of various products. However, traditional packaging materials often fall short in terms of sustainability and functionality (Ahari et al., 2022, Kong et al., 2023, Zhang et al., 2023). This has led to the development of innovative packaging solutions, such as smart and active packaging films. With advancements in technology, the packaging industry has witnessed the emergence of smart and active packaging films (Aman Mohammadi et al., Liu et al., 2021, Zheng et al., 2022). These films are designed to actively interact with the packaged product, providing additional functionalities beyond traditional packaging materials. Strengths of smart and active packaging films include their ability to extend the shelf life of perishable foods, enhanced safety through providing an additional layer of safety by incorporating halochromic that detect temperature, pressure, or gas leaks, improved product quality, and provide information and convenience to consumers (Alizadeh-Sani et al., 2020, Amin et al., 2022, Sani et al., 2023). However, these innovation technologies deal with some limitations including their higher cost compared to traditional packaging materials, technological compatibility and integration, recycling challenges, and complexity involved in their design and manufacturing (Alizadeh-Sani

et al., 2020, Siddiqui et al., 2022).

In recent years, the development of smart and active packaging films has revolutionized the packaging industry (Ahari et al., 2022, Alizadeh Sani et al., 2022). These films are designed to go beyond traditional packaging, providing additional functionalities such as improved shelf life, freshness monitoring, and enhanced safety (Alizadeh-Sani et al., 2020, Mohammadian et al., 2020). One such promising material is a film made from gelatin, pectin, and Pistacia peel anthocyanin, as investigated in this study.

Gelatin (Gel) and pectin (Pec) are commonly used in the food industry as gelling agents, emulsifiers, and stabilizers (Ye et al., 2022). When incorporated into smart/active packaging films, they provide mechanical strength, flexibility, and water/oxygen barrier properties (Aitboulahsen et al., 2020). Gelatin is a protein derived from collagen, commonly found in animal tissues. It has been widely used in the food industry for its gelling, stabilizing, and film-forming properties, thereby forming a transparent and flexible film, making it suitable for packaging applications (Dafader et al., 2016). Pectin, on the other hand, is a natural polysaccharide found in the cell walls of fruits and vegetables. It is known for its gelling and thickening capabilities (Ye et al., 2022). Both G and Pec offer excellent film-forming properties, making them ideal candidates for packaging applications.

\* Corresponding author. Dr. Hamed Ahari

E-mail address: [Dr.h.ahari@gmail.com](mailto:Dr.h.ahari@gmail.com) (H. Ahari).

<https://doi.org/10.1016/j.fochx.2024.101217>

Received 28 November 2023; Received in revised form 29 January 2024; Accepted 8 February 2024

Available online 20 February 2024

2590-1575/© 2024 The Author(s). Published by Elsevier Ltd. This is an open access article under the CC BY-NC-ND license (<http://creativecommons.org/licenses/by-nc-nd/4.0/>).

Pistachio peel anthocyanin (PSA), is a natural pigment known for its antioxidant properties. It not only adds color to the film but also enhances its functionality (Nobari et al., 2022, Sadi and Ferfera-Harrar, 2023). Anthocyanins have been shown to have antimicrobial and antioxidant properties, which can help extend the shelf life and freshness monitoring of packaged food products (Tavassoli et al., 2023). For instance, a colorimetric indicator based on butterfly pea flower anthocyanins and gelatin/pectin for shelf life detection of fish was developed and reported a strong correlation between color change and pH/TVB-N (Narayanan et al., 2023). Unfortunately, there is still a challenge in the stability and solubility properties of anthocyanins. Nanoemulsions are colloidal dispersions composed of an oily phase and an aqueous phase with a lipid droplet size of 10–100 nm (Norcino et al., 2020). The incorporation of anthocyanins loaded nanoemulsions into the films improved controlled release and stability of anthocyanins and also increased their antioxidant and antimicrobial properties (Chu et al., 2020).

Additionally, the use of natural anthocyanins reduces the reliance on synthetic additives and provides a more sustainable packaging solution (Alizadeh-Sani et al., 2020, Mohammadian et al., 2020).

The combination of gelatin, pectin, and PSAs creates a smart and active packaging film that offers several advantages. Firstly, the film is biodegradable and environmentally friendly, addressing the growing concerns about plastic waste. It can be easily disposed of without harming the environment, unlike traditional plastic films that take hundreds of years to decompose. Secondly, the film exhibits excellent mechanical and barrier properties. It has good tensile strength, flexibility, and water/oxygen barrier properties, which help preserve the freshness and quality of the packaged food. The film also provides a barrier against UV light, preventing the degradation of sensitive food components such as vitamins and flavors (Alizadeh-Sani et al., 2020, Drago et al., 2020).

Furthermore, the active properties of PSAs make the film capable of releasing antioxidants and antimicrobial agents into the packaged food. This can help inhibit the growth of spoilage microorganisms and prolong the shelf life of perishable products. The antioxidant properties of the film can also protect the food from oxidative damage, maintaining its nutritional value and sensory attributes. In addition to its functional benefits, the Gel/Pec/PSAs film offers aesthetic advantages. The natural color of the anthocyanin adds an attractive visual appeal to the packaging, enhancing the overall consumer experience. This can be particularly appealing for premium and high-value food products (Liu et al., 2021, Khezerlou et al., 2023).

Accordingly, this study aims to develop an innovative smart film by incorporating PSAs into Gel/Pec via casting method. Following, the physical, mechanical, spectroscopic, colorimetric, antioxidant, and antimicrobial properties of the films were investigated. Finally, the efficiency of the smart film and its color changes for monitoring the freshness of shrimp were investigated.

## Experimental

### Materials

The gelatin (gel strength of 200 g Bloom), pectin (Molecular Weight; 472 kDa, and esterification degree;  $\leq 67\%$ ), glycerol, Glacial acetic acid ( $\geq 99\%$ ), hydrochloric acid (HCL), sodium hydroxide (NaOH), and methanol were provided from Merk (Darmstadt, Germany). Pistachio (*Pistacia vera* L.) of the Akbari variety was bought from Rafsanjan city (Kerman, Iran). The green peels from the pistachio were removed and dried in the shade and then smashed through a mill (particle size up to 2 mm). Fresh shrimp (*Litopenaeus vannamei*) were bought from seafood sales center (Tehran, Iran). The rest chemical reagents were analytical reagents.

### Extraction of pistachio peel anthocyanins (PSAs)

The soaking and ultrasound methods were used to extract pistachio peel anthocyanins. In the first method, 100 g of smashed pistachio peels was added to 1000 mL solvent (methanol/1% HCL) and incubated for 2 h at 25, 50, and 75 °C in a shaker incubator to complete extraction (Martorana et al., 2013). In the second method, 100 g of pistachio peel powders were dissolved in methanol/1%HCL and then sonicated for 20 min at 25 °C and powers 100, 200, 300, and 400 W (Nadernejad et al., 2013). Finally, the mixtures were centrifuged at 3000 rpm for 20 min and the supernatant was collected and concentrated by rotary evaporator at 50 °C. The resulting extracts were held in the refrigerator at 4 °C for future application.

For anthocyanin content estimation, 0.1 g of fresh extract was added separately to 10 mL methanol solution and methanol/HCL (99:1) solution and incubated at 25 °C in the dark for 24 h. After that, the mixture was centrifuged for 10 min at 4000 rpm and the absorbance of the supernatant solution was measured at 530 nm (Nadernejad et al., 2013). The anthocyanin content was expressed as  $\mu\text{mol/g}$  wet weight with the help of the following equations:

$$A = \epsilon bc \quad (1)$$

Here, A is the absorbance of a pigment solution,  $\epsilon$  is the molar absorption coefficient (3300  $\text{cm}^2/\text{M}$ ), b is the length of the path passed by the light (cm), and c is the concentration of the solution (M).

### PSAs-nanoemulsion preparation

The nanoemulsion was prepared according to Artiga-Artigas et al. (2018). First, pectin solutions were prepared by dissolving 3 % in water at 70 °C for 2 h and held overnight at 4 °C to complete hydration. Then, the pectin solution was mixed with anthocyanin and blended at 9600 rpm for 2 min, which led to the formation of a coarse emulsion. Finally, nanoemulsions were formed by passing the coarse emulsion via a microfluidizer (Kika-labortechnik, Germany) at 150 MPa for 5 cycles. PSAs-nanoemulsions were cooled at the outlet of the microfluidization unit by an external coil immersed in a water bath with ice.

### Preparation of halochromic films

The halochromic films were obtained based on the methodology described by Jridi et al. (2020), through the casting technique. First, 0.3 g of pectin, 0.3 g of gelatin, and 0.09 g of glycerol were dissolved in 200 mL of distilled water with continuous magnetic stirring at 40 °C for 30 min. To prepare composite films, pectin and gelatin at different ratios (w/w%) were mixed with PSAs according to Table S1, and then slowly homogenized. The compositions of pure or composite films were: 100 % Gel = T1, 99 % Gel/1% PSAs = T2, 89 % Gel/10 % Pec/1% PSAs = T3, and 79 % Gel/20 % Pec/1% PSAs = T4. Finally, the film-forming solutions (25 mL) were poured on a Petri dish (6 cm  $\times$  6 cm). Then, films were dried at 25 °C and RH of 50 % for 48 h.

### Characterization of halochromic films

#### Structural analysis

The chemical bond structure of halochromic films was studied by a Shimadzu Fourier transform infrared (FTIR) spectrometer (Shimadzu, Japan) in the range of 400–4000  $\text{cm}^{-1}$  at a resolution of 4  $\text{cm}^{-1}$ . X-ray diffraction (XRD) patterns of halochromic film samples were taken with the TA-instrument (USA) X-ray diffractometer in a  $2\theta$  range of 10° to 80° with Cu-K $\alpha$  radiation.

#### Morphological and thermal analysis

The surface morphology of the halochromic film samples was characterized by Zwick scanning electron microscopy (SEM, Zwick,

Germany). Before imaging, the film samples were dispersed in glutaraldehyde and acetonitrile solutions and then coated with gold after evaporation of solvents. The glass transition temperature of halochromic film samples was measured by a differential scanning calorimeter (DSC, Shimadzu, Japan). A heating rate of 10 °C/min from 0 to 200 °C was used for the film specimens with a weight of almost 4 mg.

#### Physical properties

**Thickness;** A hand-held micrometer (Mitutoyo, Japan) with an accuracy of 0.001 mm was applied to measure the thickness of each halochromic film sample from 3 different points.

**Moisture content (MC);** The weighed sample of halochromic films ( $W_1$ ) was dried at 105 °C for 24 h ( $W_2$ ), and the MC of the films was ascertained by the weight difference of films before and after drying, with the assistance of the following equations:

$$MC(\%) = (W_1 - W_2/W_1) \times 100 \quad (2)$$

**Solubility in water (WS);** 0.6 g of each film sample was placed in a desiccator involving P<sub>2</sub>O<sub>5</sub> (0 % RH at 40 °C for 24 h) ( $W_1$ ). Then each film was immersed in 100 mL of deionized water at 25 °C for 24 h with continuous stirring. Finally, the residue of films filtrated and dried at a temperature of 40 °C ( $W_2$ ), with the aid of the following equations:

$$WS(\%) = (W_1 - W_2/W_1) \times 100 \quad (3)$$

**Optical properties;** The light transmittance spectra of halochromic film samples were determined by a Varian spectrophotometer (Model Conc 50, Hitachi, Japan).

**Color parameter of the halochromic films;** The halochromic films were cut into squares of 2 cm in size and dissolved in a buffer solution (2 mL) with pH = 1.0–14.0 adjusted with HCl and NaOH. The color change ( $L$  (light),  $a$  (red/green), and  $b$  (yellow/blue)) of halochromic films were analyzed by a Hunter-Lab (LanYuXuan, Guangdong, China). The total color difference ( $\Delta E$ ) was obtained with the help of the formula:

$$\Delta E = \sqrt{(\Delta L)^2 + (\Delta a)^2 + (\Delta b)^2} \quad (4)$$

#### Gas barrier performances

**Water vapor permeability (WVP);** The halochromic films' permeability to water vapor was determined according to ASTM E96-05 standard method. The film samples were fixed tightly on the cup containing water (100 % RH = relative humidity), which were put into a desiccator involving silica gel (0 % RH). Every 2 h, the cups were weighed to reach to constant weight.

**Oxygen permeability (OP);** Mocon Ox-Tran 21.2 was used to estimate the O<sub>2</sub> transmission rate (at 25 °C, 50 % RH, and 21 % O<sub>2</sub>) through the halochromic films with the ASTM method Standard D 3985. The halochromic films were put into a stainless-steel mask with an open testing area of 5 cm<sup>2</sup>. Using a carrier gas (N<sub>2</sub>/H<sub>2</sub>), oxygen is passed through the calorimetric sensor.

#### Mechanical properties

Tensile tests of halochromic films were carried out by a tensile testing machine (Brookfield, USA) under the following conditions: size (length: 70 mm, width: 10 mm); test speed: 50 mm/min; initial grip distance: 50 mm.

#### Application of halochromic film on shrimp preservation

Shrimp samples with uniform weight (20 g) were placed in a plastic petri dish, and different films (T1, T2, T3, T4) were applied to seal the petri dish. The pH was measured through a digital pH meter (Metrohm, Switzerland). The total volatile basic nitrogen (TVB-N) values of the shrimp samples were investigated according to the method described by Li et al. (2012). The total viable counts (TVC) and total psychrophiles count (TPC) of shrimps were measured through the standard plate count

method (Yun et al., 2022).

#### Data analysis

Each experiment was performed at least in triplicate. All the data were carried out by SPSS-21 (IBM Corp., USA) and reported as mean ± standard deviation by using Duncan's test ( $P < 0.05$ ), and analysis of variance (one-way ANOVA).

## Results and discussion

### Characterization of the halochromic films

#### Morphological properties

The morphology of the surface of fabricated different films was determined by SEM. From Fig. 1a, a uniform and smooth surface without particles has been observed in T1 film. This behavior can be associated with the high purity of Gel and the absence of secondary phases in this sample. In Fig. 1b, it was observed the particles with a size of 0.76 μm which was caused by the presence of anthocyanins. As shown in Fig. 1c and d, with the addition of Pec into the matrix, the number and size of particles visibility on the surface increased, so that the particle size was 0.8 μm and 1.71 μm for T3 and T4 films, respectively. In large amounts of pectin, the network formation between pectin and gelatin networks is limited, resulting in weak compact structures (Candra et al., 2023).

Variation of this sort in film morphology have been reported after addition of blueberries anthocyanins into zein (Kong et al., 2023), *Hibiscus sabdariffa* L. anthocyanins into chitosan (Khezerlou et al., 2023), and barberry/saffron anthocyanins into gelatin/chitosan nanofibers (Tavassoli et al., 2022).

#### Crystallinity of the films

The XRD patterns of the T1, T2, T3, and T4 films are shown in Fig. 2A. For T1 film, there were two peaks at 20.8° and 37.9°, which was related to T1 having a semi-crystalline nature resulting from its triple helical and α-helix structure (Khezerlou et al., 2023, Khezerlou et al., 2023). T2 films showed similar patterns to T1 film, was probably because the PSAs' good compatibility with T1 film. In the XRD pattern of T3 film, a new peak near 43.9° was visible, due to the amorphous state of the Pec, which agreed with the results reported by (Mellinas et al., 2020, Zarandona et al., 2021). Additionally, the wide diffraction peak of T4 films at 43.9° moved to 38.5°. This may be related to the hydrogen bond between Pec and Gel. Therefore, XRD results can prove the blending of anthocyanin and Pec with Gel formed a favorable semi-crystalline structure.

#### Chemical groups/interactions

The FTIR spectra of the T1, T2, T3, and T4 films are shown in Fig. 2B. In the spectrum of Gel film, the peaks at 3348, 3198, 1633, 1514, 1464, and 631 cm<sup>-1</sup> arise from the O—H stretching, N—H stretching, O—H bending, N—H bending, —CH<sub>2</sub> bending, and rocking vibrations of —CH<sub>2</sub> bonds, respectively (Tavassoli et al., 2022). In addition, the peaks observed at 2947, 1590, and 1167 cm<sup>-1</sup> are related to C—H stretching vibration, C=C stretching vibration, and C—OH stretching vibration in the Gel structure (Han and Song, 2021, Ye et al., 2022). The spectrum of T2 smart film showed peaks at 1632 cm<sup>-1</sup>, and this peak can be due to the presence of anthocyanin in the structure (with several OH groups) (Rawdkuen et al., 2020). The intensity of peaks of T3 film at wave-numbers 3205, 1520, and 1210 cm<sup>-1</sup> decreased by adding Pec, proving the reduction of Gel amount in the composite (Guo et al., 2021). It has also been observed that with the increase of Pec amount, the intensity of the peaks of 3423, 1630, 1190, and 1090 cm<sup>-1</sup> increased. The peaks appeared in the spectra of the T4 films at about 2930 and 2845 cm<sup>-1</sup>, owing to C—H symmetric and asymmetric stretching vibration. The shift of the peak related to O—H stretching and bending vibrations in the presence of Pec also confirms the formation of H-bonds between the OH



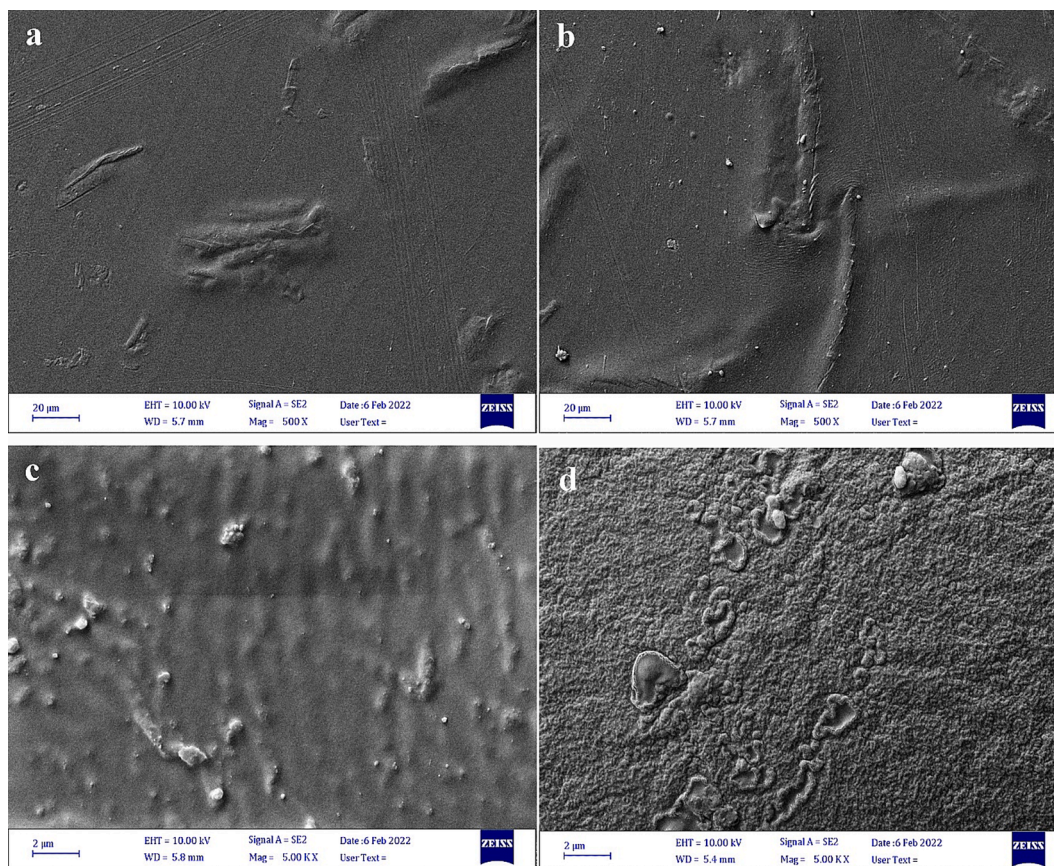


Fig. 1. Surface SEM images of (a) T1, (b) T2, (c) T3, and (d) T4.

groups in the Gel structure and the polar groups in the Pec structure.

#### Thermal properties

Thermal analyses provide information not only about thermal properties but also about the structure of materials. The Differential scanning calorimetry (DSC) thermogram of pure gelatin film and composite films is shown in Fig. 2C. According to this thermal profile, an endothermic process is observed at a temperature of about 74.6 °C, and this peak is related to the glass transition temperature ( $T_g$ ) in the amorphous regions of biopolymer, which is caused by the micro-Brownian motion of the main chain (Dafader et al., 2016). Also, in this temperature range, the endothermic peak associated with the melting of the triple helix crystal structure occurs. The enthalpy of this stage is about 66.5 J/g with a starting temperature of about 61.84 °C. Two other endothermic peaks appeared at 173.3 °C and 243.4 °C, with starting temperatures of 156.2 °C and 212.9 °C, and enthalpies of 5.5 J/g and 50.9 J/g, respectively. Finally, an exothermic peak can be seen in the DSC profile of pure gelatin at a temperature of about 280 °C. By adding PSAs (1 %) to the film matrix (T4 film), changes have been created in the DSC thermogram of the composite films compared to T1 film. In the DSC profile of the smart film containing PSAs (T4 film), the starting and process temperatures of the first stage have been shifted from 74.6 °C and 61.8 °C to 81.7 °C and 44.7 °C, respectively, according to the enthalpy changes of this stage, as it is increased from about 66.5 J/g to about 101.5 J/g. This demonstrates the impact of anthocyanin on the thermal stability of the smart film. Additionally, the presence of anthocyanin causes a change in the structure, resulting in the second stage peak becoming invisible. This change can be attributed to the interaction between anthocyanin and the film. Furthermore, the inclusion of anthocyanin in the film matrix eliminates the exothermic peak associated with temperature degradation, further highlighting the significant influence of anthocyanin on the gelatin structure. When

different amounts of pectin are added to the film structure, the same two broad peaks can be observed, accompanied by smaller peaks. These observations indicate that increasing the concentration of pectin in the film matrix promotes both the temperature and enthalpy of the process (Azizah et al., 2023).

In other words, creating a hydrogen bond between the functional groups in Pec and the polar compounds in the film matrix increases the thermal stability of the composite. Also, strengthening the interactions between Pec-Gel by increasing the concentration of Pec in the structure has led to an increase in the amount of energy required for the thermal decomposition of the composite (Lin et al., 2023). This increase in the energy required to break the hydrogen bonds between Pec and Gel can also confirm the results of the XRD pattern, where it was also observed that increasing the concentration of Pec (T4 film) caused an increase in the degree of crystallinity of the structure. Many studies have observed similar changes with the addition of Pec and anthocyanin to the matrix of smart films (Zheng et al., 2022, Ahammed et al., 2023, Lin et al., 2023).

#### Physical properties

**Thickness:** As reported in Table 1, no significant statistical difference was observed in the thickness of films ( $P > 0.05$ ) and the samples showed a thickness of about 0.202 mm. However, the increase of dry matter by adding nanomaterials, bioactives, etc., in the film matrix may increase the thickness of the films (Khezerlou et al., 2023).

**Opacity:** According to the results (Table 1), the highest opacity was observed for T3 and T4 films with an opacity equal to 0.05 % ( $P \leq 0.05$ ). While the opacity value for T1 film and T2 were 0.02 and 0.04 %, respectively.

**Solubility in water (WS):** In this study, the highest solubility in water was observed in the T1 film (73.98 %), the lowest solubility belonged to

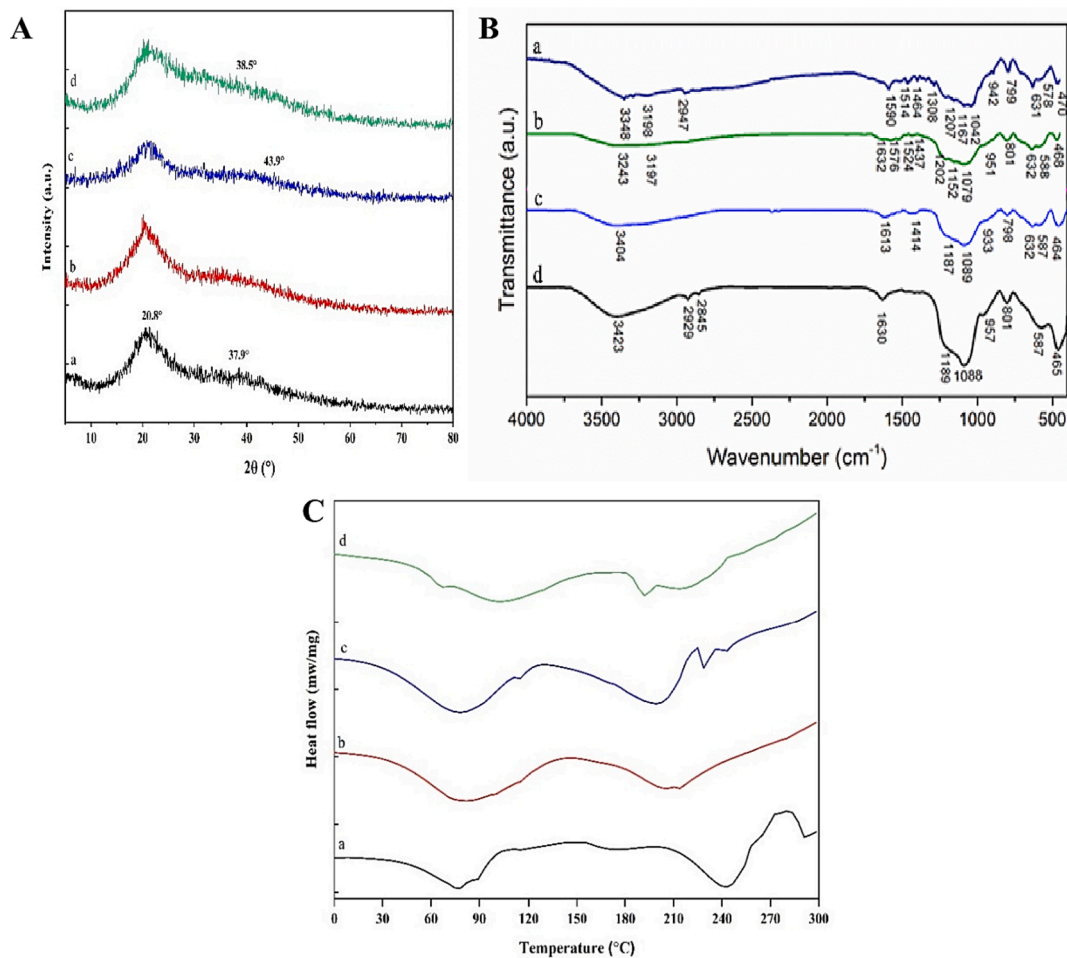


Fig. 2. The XRD pattern (A), FT-IR spectra (B), and DSC curve (C) of packaging films; (a) T1, (b) T2, (c) T3, and (d) T4 film.

Table 1

Physical properties of gelati-based packaging films containing pectin and anthocyanin.

Films	Thickness (mm)	Opacity (%)	WS (%)	MC (%)	WVP ( $\text{g}\cdot\text{s}^{-1}\cdot\text{Pa}^{-1}\cdot\text{m}^{-1}$ )	OP ( $\text{meq}/\text{kgO}_2$ )
T1	0.202 ± 0.50 <sup>b</sup>	0.02 ± 0.0 <sup>b</sup>	73.98 ± 0.36 <sup>a</sup>	88.14 ± 0.12 <sup>a</sup>	2.81 ± 0.0 <sup>a</sup>	5.25 ± 0.02 <sup>a</sup>
T2	0.202 ± 0.39 <sup>ab</sup>	0.04 ± 0.0 <sup>b</sup>	73.18 ± 0.20 <sup>b</sup>	87.48 ± 0.22 <sup>b</sup>	2.72 ± 0.0 <sup>c</sup>	5.13 ± 0.05 <sup>b</sup>
T3	0.202 ± 0.23 <sup>ab</sup>	0.05 ± 0.0 <sup>ab</sup>	72.11 ± 0.20 <sup>c</sup>	86.85 ± 0.16 <sup>c</sup>	2.70 ± 0.0 <sup>d</sup>	4.26 ± 0.05 <sup>d</sup>
T4	0.202 ± 0.20 <sup>a</sup>	0.05 ± 0.0 <sup>a</sup>	72.53 ± 0.23 <sup>c</sup>	86.94 ± 0.27 <sup>c</sup>	2.74 ± 0.0 <sup>b</sup>	4.70 ± 0.10 <sup>c</sup>

Gel: gelatin, Pec: pectin, PSAs: pistachio peel anthocyanin, WS: solubility in water, SI: Swelling Index, WVP: water vapor permeability, OP: oxygen permeability. The values are presented as a mean ± SD. In the same column, any two means, followed by the same lowercase letters, are not significantly different ( $P > 0.05$ ) by Duncan's multiple range tests.

the nanocomposite film of T3 (72.11 %) and the T4 nanocomposite film (72.53 %). As recent studies have indicated, the addition of nanomaterials, and bioactive compounds such as essential oils/extracts, and pigments, slightly decreases the water solubility of packaging films, which is caused by the interaction of film ingredients (Etxabide et al., 2021).

**Moisture content (MC):** Similar to the solubility results, T3 film and T4 films displayed the lowest MC values (86.94 % and 86.85 %) and T1 film

showed the highest MC value (88.14 %) (see Table 1). The incorporation of PSAs significantly decreased the T1 films' MC (87.48 %). Strong interactions between film components and the reduction of free functional groups to interact with water molecules are the mechanisms for reducing the MC in composite films, and this phenomenon has been reported by several studies (Yong and Liu, 2020, Qin et al., 2021).

**Water vapor permeability (WVP):** The WVP of the T1 film was  $2.81 (\text{g}\cdot\text{s}^{-1}\cdot\text{Pa}^{-1}\cdot\text{m}^{-1})$ , and the addition of PSAs reduced the WVP of the T2 film ( $2.72 \text{g}\cdot\text{s}^{-1}\cdot\text{Pa}^{-1}\cdot\text{m}^{-1}$ ). The results of WVP show that films T4 ( $2.74 \text{g}\cdot\text{s}^{-1}\cdot\text{Pa}^{-1}\cdot\text{m}^{-1}$ ) and T3 ( $2.70 \text{g}\cdot\text{s}^{-1}\cdot\text{Pa}^{-1}\cdot\text{m}^{-1}$ ) had lower permeability compared to T1 film (see Table 1). As expected, with the addition of anthocyanin and pectin, the water vapor permeability of the gelatin film decreased. The OH group in natural pigment and the functional groups of gelatin or pectin may create a H-bond. It was thus harder for water molecules to pass through the color film because the network structure of the composite films was more compact and had less empty space. Additionally, it's possible to block the microchannel in the film network, which would lower the polymer matrix's tendency to water (Duan et al., 2022, Liu et al., 2022). Various studies also showed that the addition of anthocyanins of blueberry (Liu et al., 2022), saffron/barberry (Tavassoli et al., 2022), eggplant (Wang et al., 2023), and raspberry (Duan et al., 2022) reduced the permeability of smart films.

**Oxygen permeability (OP):** The OP of the composite films exhibited the same trend as the changes in the water permeability. As reported in Table 1, the OP value was  $4.26 (\text{meq}/\text{kgO}_2)$  and  $4.70 (\text{meq}/\text{kgO}_2)$  for T3 and T4 colorimetric films respectively, and  $5.25 (\text{meq}/\text{kgO}_2)$  for T1 film. After addition of PSAs, a noticeable fall in the OP value has been observed. These results revealed that PSAs significantly reduced the



permeability of films to moisture and oxygen. Similar to changes in WVP values, the addition of various anthocyanins such as *Loropetalum chinense* var. *rubrum* (Zheng et al., 2022) and blueberries (Kong et al., 2023) decreased the oxygen permeability in smart films. These changes can be attributed to the compact and dense structure of the composite films.

### Mechanical properties

In addition to physical properties, mechanical properties also play a very important role in the development of packaging materials. As presented in Table 2, T1 film had the lowest amount of elongation at break (flexibility, 49.96 %) and tensile strength (0.62 MPa), while the highest quantity of flexibility (56 %) and strength (0.70 MPa) was obtained for T4 colorimetric film. On the other hand, the highest value of Young's modulus was observed for film T2 (14.20 MPa) and the lowest value for T4 (12.54 MPa). This reduce in modulus may be related to the plasticizing impact of glycerol (Lal et al., 2021). These results show the positive effect of pigment addition on mechanical properties. For example, Yun et al. (2022), reported that by increasing the concentration of *Loropetalum chinense* var. *rubrum* anthocyanin, the tensile strength of the smart films increased from 27.25 MPa to 28.20 MPa. While the flexibility of their films decreased from 60.18 % to 58.96 % (Zheng et al., 2022). In another study, it was proved that the tensile strength (TS) of zein film significantly increased after the addition of blueberry anthocyanin and the flexibility of the films did not change significantly. It was believed that the formation of intermolecular interactions between anthocyanin and zein, such as hydrogen bonding, was the reason of the zein film's increased TS (Kong et al., 2023).

### Color properties

Another important characteristic of smart films is their color changes at different pHs, which are investigated by color indices ( $L$  (lightness),  $a$  (redness),  $b$  (yellowness)). Visual observation of the color change of PSAs solution (Fig. 3A) and smart films containing anthocyanin (Fig. 3B) at different pH exhibited that with changes in pH from 1 to 14, their color changed from cherry/pink to yellow and brown so color changes in acidic to neutral pH ( $\text{pH} = 1\text{--}6$ ) was from cherry to pink, and in alkaline conditions, it changed to yellow and brown. These color changes are caused by the transformation in the structure of anthocyanins at different pHs so that the yellow color appears with the formation of the chalcone structure at alkaline pHs. As reported in Table S4, the  $L$  value of the films decreased significantly with increasing pH. So, in films containing PSAs, the lowest  $L$  was observed at 13, and 14 pHs (23.05, and 25.50) compared to T1 film (75.79, and 75.72), and higher  $L$  values showed in acidic pHs. Also,  $a$  value (redness) increased in films containing PSAs under acidic conditions ( $\text{pH} = 1$ ) due to the appearance of a reddish color and reached to 35.63 for T4 film. While  $a$  value was equal to 0.78 for T1 film. However, with increasing pH, the  $a$  index decreased for smart films and increased for T1 films (see Table S5). On the other

**Table 2**

Mechanical properties of gelatin-based packaging films containing pectin and anthocyanin.

Films	TS (MPa)	EAB (%)	YM (MPa)
T1	0.62 ± 0.00 <sup>c</sup>	46.96 ± 0.25 <sup>c</sup>	13.25 ± 0.10 <sup>ab</sup>
T2	0.66 ± 0.01 <sup>b</sup>	46.51 ± 1.09 <sup>c</sup>	14.20 ± 0.09 <sup>a</sup>
T3	0.67 ± 0.02 <sup>ab</sup>	51.25 ± 3.59 <sup>b</sup>	13.27 ± 0.70 <sup>ab</sup>
T4	0.70 ± 0.01 <sup>a</sup>	56.00 ± 3.56 <sup>a</sup>	12.54 ± 1.13 <sup>b</sup>

Gel: gelatin, Pec: pectin, PSAs: pistachio peel anthocyanin, TS: tensile strength, EAB: elongation at break, YM: Young's modulus. The values are presented as a mean ± SD. In the same column, any two means, followed by the same lower-case letters, are not significantly different ( $P > 0.05$ ) by Duncan's multiple range tests.

hand,  $b$  values (yellowness) increased with increasing pH for T1 film and reached 3.67 at pH 14. However, the  $b$  parameter was the highest value for smart films in the range of pH 6–8 (see Table S6). Color changes and similar behaviors have been reported after the addition of various anthocyanins such as *Loropetalum chinense* var. *rubrum* petals (Zheng et al., 2022), *Lycium ruthenicum* (Qin et al., 2021), *Hibiscus sabdariffa* L. (Khezerlou et al., 2023), and blueberry (Liu et al., 2022) in different matrices.

### Application in shrimp monitoring and preservation

In this study, the T4 film was selected to monitor the shrimp freshness. As shown in Fig. S4, the color of the film starts to change at refrigerator temperature at 24 h, showing the shrimps begin to spoilage along with the color change of film from pink to cinnamon color. Moreover, the T4 film as the halochromic alters to brown after 72 h, indicating the shrimp spoilage. Khezerlou et al. (2023) used sumac anthocyanin as an halochromic of shrimp, Khezerlou et al. (2023) also used *hibiscus sabdariffa* anthocyanin as an halochromic of fish fillet, and Mohseni-Shahri and Moeinpour (2023) used it for shrimp freshness. The color changes of the smart film in this study were similar to the color changes of the films reported in recent studies.

To preserve shrimp, changes in pH, TVB-N, TVC, and TPC in the fabricated films were evaluated on days 0, 3, and 7 days of storage at 4 °C (Table 3). Shrimp stored by T1 films showed the highest pH on the 7th, probably due to the production of volatile compounds by spoilage bacteria on the surface of shrimp (Ye et al., 2022). The T4 stored shrimp showed the lowest pH on the 7th, which can be owing to the antibacterial activity of the films after the addition of PSAs. In addition, the TVB-N values of shrimp were also raised during storage, which was due to proteins decomposing by bacteria proteolytic (Chi et al., 2023). It should be noted that the TVB-N values of T4 changed slowly (on the 7th). The antibacterial performance of the packaging films was assessed by measuring the TVC and TPC of shrimp with different halochromic films on the 7th day of storage. The shrimp stored in T1 had the largest TVA and TPC, while T4 film stored shrimp had the lowest TVC and TPC owing to the antibacterial effect of PSAs. In conclusion, the T4 films slowed the pH increase, TVB-N increase, and microbial growth of shrimp, which will greatly extend the shelf life of shrimp.

### Conclusion

A recent study has revealed that colorimetric labels made from natural pigments (Pistachio peel anthocyanins) and polymers (gelatin/pectin) can be used to monitor the quality of shrimp during storage. These labels change color in response to changes in pH and the presence of ammonia gas inside the packaging. Spectroscopy analysis indicated that the pigments were successfully incorporated into the gelatin/pectin matrix of the labels. The addition of anthocyanins enhanced the labels' mechanical strength by crosslinking the gelatin/pectin molecules. Additionally, the anthocyanins reduced the oxygen permeability and water vapor permeability of the gelatin films, likely due to their cross-linking properties. The color change of the pigments depends on pH and the presence of volatile nitrogenous gases, making them suitable for monitoring seafood spoilage. This was verified by tracking the freshness of shrimp during storage using gelatin/pectin labels that were loaded with PSAs. As storage time increased, the labels' color changed from pink (fresh) to yellow (spoiled). The degree of color shift was closely correlated with TVB-N and pH values. These natural sensors have potential applications in the food industry, offering real-time information about the freshness of food products for producers, retailers, and consumers. The use of such smart packaging materials can contribute to sustainability and address environmental concerns in the food industry.

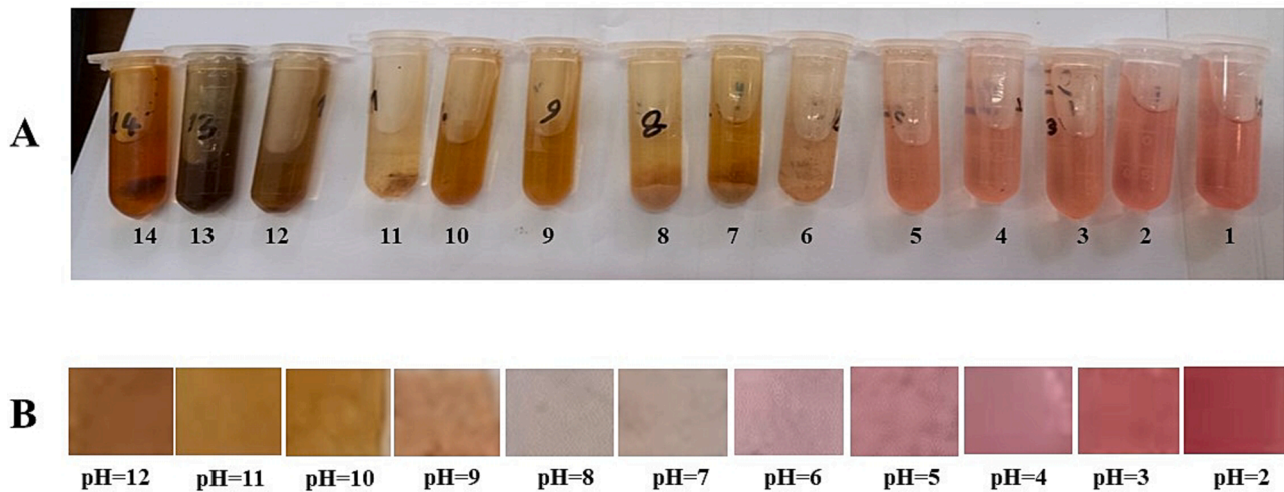


Fig. 3. Visual observation of the color changes of PSAs solution (A) and smart films (B) at different pH.

Table 3

The pH, TVB-N, TVC, and TPC changes in shrimp during storage at 4 °C.

Films	Time (Day)	pH	TVB-N (mg /100 g of meat)	TVC (log10CFU/g)	TPC (log10CFU/g)
T1	0	5.4 ± 0.00 <sup>aA</sup>	3.5 ± 0.00 <sup>aA</sup>	4.28 ± 0.01 <sup>aA</sup>	3.16 ± 0.03 <sup>aA</sup>
	3	5.51 ± 0.01 <sup>aA</sup>	9.33 ± 0.40 <sup>aA</sup>	5.70 ± 0.03 <sup>aA</sup>	5.38 ± 0.01 <sup>aA</sup>
	7	5.73 ± 0.01 <sup>aA</sup>	12.6 ± 0.70 <sup>aA</sup>	6.8 ± 0.02 <sup>aA</sup>	6.64 ± 0.05 <sup>aA</sup>
T2	0	5.4 ± 0.00 <sup>aA</sup>	3.5 ± 0.00 <sup>aA</sup>	4.28 ± 0.01 <sup>aA</sup>	3.13 ± 0.05 <sup>aA</sup>
	3	5.43 ± 0.01 <sup>bA</sup>	8.63 ± 0.40 <sup>aA</sup>	5.40 ± 0.01 <sup>bA</sup>	5.19 ± 0.00 <sup>bA</sup>
	7	5.68 ± 0.01 <sup>bA</sup>	11.2 ± 0.70 <sup>bA</sup>	6.34 ± 0.00 <sup>bA</sup>	6.13 ± 0.02 <sup>bA</sup>
T3	0	5.4 ± 0.00 <sup>aA</sup>	3.5 ± 0.00 <sup>aA</sup>	4.27 ± 0.02 <sup>aA</sup>	3.14 ± 0.04 <sup>aA</sup>
	3	5.41 ± 0.01 <sup>cA</sup>	7.46 ± 0.40 <sup>bA</sup>	5.27 ± 0.03 <sup>cA</sup>	4.99 ± 0.02 <sup>cA</sup>
	7	5.58 ± 0.01 <sup>cA</sup>	10.03 ± 0.80 <sup>bA</sup>	6.02 ± 0.02 <sup>cA</sup>	5.89 ± 0.02 <sup>cA</sup>
T4	0	5.4 ± 0.00 <sup>aA</sup>	3.5 ± 0.00 <sup>aA</sup>	4.28 ± 0.01 <sup>aA</sup>	3.16 ± 0.02 <sup>aA</sup>
	3	5.41 ± 0.00 <sup>bA</sup>	6.53 ± 0.40 <sup>cA</sup>	5.11 ± 0.02 <sup>dA</sup>	4.84 ± 0.01 <sup>dA</sup>
	7	5.54 ± 0.01 <sup>dA</sup>	8.63 ± 0.40 <sup>cA</sup>	5.83 ± 0.02 <sup>dA</sup>	5.64 ± 0.08 <sup>aA</sup>

TVB-N: total volatile basic nitrogen; TVC: total viable counts; TPC: total psychrophiles count. Gel: gelatin, Pec: pectin, PSAs: pistachio peel anthocyanin. The values are presented as a mean ± SD. In the same column, any two means, followed by the same lowercase letters, are not significantly different ( $P > 0.05$ ) by Duncan's multiple range tests.

#### CRedit authorship contribution statement

**Alireza Taheri-Yeganeh:** Writing – original draft, Methodology, Conceptualization. **Hamed Ahari:** Writing – review & editing, Methodology, Investigation, Funding acquisition, Conceptualization. **Zohreh Mashak:** Validation, Supervision, Investigation, Conceptualization. **Seid Mahdi Jafari:** Writing – review & editing, Visualization, Software, Investigation, Conceptualization.

#### Declaration of competing interest

The authors declare that they have no known competing financial interests or personal relationships that could have appeared to influence

the work reported in this paper.

#### Data availability

The data that has been used is confidential.

#### Acknowledgements

The authors special thanks to Nano Research Lab-ultrasonic Section, Islamic Azad University, Tehran, Iran.

#### Appendix A. Supplementary data

Supplementary data to this article can be found online at <https://doi.org/10.1016/j.fochx.2024.101217>.

#### References

- Ahmed, S., Easani, M., Liu, F., & Zhong, F. (2023). Encapsulation of Tea Polyphenol in Zein through Complex Coacervation Technique to Control the Release of the Phenolic Compound from Gelatin-Zein Composite Film. *Polymers*, 15(13), 2882.
- Ahari, H., G. Karim, S. A. Anvar, S. Paidari, S. A. Mostaghim and A. S. Mazinani (2022). Method for producing antimicrobial nanofilms packaging cover based on titanium nano-dioxide through extrusion for extension of food shelf-life, Google Patents.
- Aitboulahsen, M., El Galiou, O., Laglaoui, A., Bakkali, M., & Hassani Zerrouk, M. (2020). Effect of plasticizer type and essential oils on mechanical, physicochemical, and antimicrobial characteristics of gelatin, starch, and pectin-based films. *Journal of Food Processing and Preservation*, 44(6), e14480.
- Alizadeh-Sani, M., Mohammadian, E., Rhim, J.-W., & Jafari, S. M. (2020). pH-sensitive (halochromic) smart packaging films based on natural food colorants for the monitoring of food quality and safety. *Trends in Food Science & Technology*, 105, 93–144.
- Alizadeh Sani, M., Khezerlou, A., Tavassoli, M., Mohammadi, K., Hassani, S., Ehsani, A., & McClements, D. J. (2022). Bionanocomposite Active Packaging Material Based on Soy Protein Isolate/Persian Gum/Silver Nanoparticles; Fabrication and Characteristics. *Colloids and Interfaces*, 6(4), 57.
- Amin, U., Khan, M. K. I., Maan, A. A., Nazir, A., Riaz, S., Khan, M. U., Sultan, M., Munekata, P. E., & Lorenzo, J. M. (2022). Biodegradable active, intelligent, and smart packaging materials for food applications. *Food Packaging and Shelf Life*, 33, Article 100903.
- Artiga-Artigas, M., Guerra-Rosas, M. I., Morales-Castro, J., Salvia-Trujillo, L., & Martín-Belloso, O. (2018). Influence of essential oils and pectin on nanoemulsion formulation: A ternary phase experimental approach. *Food Hydrocolloids*, 81, 209–219.
- Azizah, F., Nursakti, H., Ningrum, A., & Supriyadi, (2023). Development of Edible Composite Film from Fish Gelatin-Pectin Incorporated with Lemongrass Essential Oil and Its Application in Chicken Meat. *Polymers*, 15(9), 2075.
- Candra, A., Tsai, H.-C., Saragi, I. R., Hu, C.-C., Yu, W.-T., Krishnamoorthi, R., Hong, Z.-X., & Lai, J.-Y. (2023). Fabrication and characterization of hybrid eco-friendly high methoxyl pectin/gelatin/TiO<sub>2</sub>/curcumin (PGTC) nanocomposite biofilms for salmon fillet packaging. *International Journal of Biological Macromolecules*, 232, Article 123423.

- Chi, W., Liu, W., Li, J., & Wang, L. (2023). Simultaneously realizing intelligent color change and high haze of  $\kappa$ -carrageenan film by incorporating black corn seed powder for visually monitoring pork freshness. *Food Chemistry*, 402, Article 134257.
- Chu, Y., Cheng, W., Feng, X., Gao, C., Wu, D., Meng, L., Zhang, Y., & Tang, X. (2020). Fabrication, structure and properties of pullulan-based active films incorporated with ultrasound-assisted cinnamon essential oil nanoemulsions. *Food Packaging and Shelf Life*, 25, Article 100547.
- Dafader, N. C., Rahman, S. T., Rahman, W., Rahman, N., Manir, M., Alam, M., Alam, J., & Sumi, S. A. (2016). Preparation of gelatin/poly (vinyl alcohol) film modified by methyl methacrylate and gamma irradiation. *International Journal of Polymer Analysis and Characterization*, 21(6), 513–523.
- Drago, E., Campardelli, R., Pettinato, M., & Perego, P. (2020). Innovations in smart packaging concepts for food: An extensive review. *Foods*, 9(11), 1628.
- Duan, A., Yang, J., Wu, L., Wang, T., Liu, Q., & Liu, Y. (2022). Preparation, physicochemical and application evaluation of raspberry anthocyanin and curcumin based on chitosan/starch/gelatin film. *International Journal of Biological Macromolecules*, 220, 147–158.
- Extabide, A., Maté, J. I., & Kilmartin, P. A. (2021). Effect of curcumin, betanin and anthocyanin containing colourants addition on gelatin films properties for intelligent films development. *Food Hydrocolloids*, 115, Article 106593.
- Guo, Z., Ge, X., Li, W., Yang, L., Han, L., & Yu, Q.-L. (2021). Active-intelligent film based on pectin from watermelon peel containing beetroot extract to monitor the freshness of packaged chilled beef. *Food Hydrocolloids*, 119, Article 106751.
- Han, H.-S., & Song, K. B. (2021). Antioxidant properties of watermelon (*Citrullus lanatus*) rind pectin films containing kiwifruit (*Actinidia chinensis*) peel extract and their application as chicken thigh packaging. *Food Packaging and Shelf Life*, 28, Article 100636.
- Jridi, M., Abdelhedi, O., Salem, A., Kechaou, H., Nasri, M., & Menchari, Y. (2020). Physicochemical, antioxidant and antibacterial properties of fish gelatin-based edible films enriched with orange peel pectin: Wrapping application. *Food Hydrocolloids*, 103, Article 105688.
- Khezerlou, A., Alizadeh Sani, M., Tavassoli, M., Abedi-Firoozjah, R., Ehsani, A., & McClements, D. J. (2023). Halochromic (pH-Responsive) Indicators Based on Natural Anthocyanins for Monitoring Fish Freshness/Spoilage. *Journal of Composites Science*, 7(4), 143.
- Khezerlou, A., Tavassoli, M., Alizadeh-Sani, M., Hashemi, M., Ehsani, A., & Bangar, S. P. (2023). Multifunctional food packaging materials: Lactoferrin loaded Cr-MOF in films-based gelatin/ $\kappa$ -carrageenan for food packaging applications. *International Journal of Biological Macromolecules*, 251, Article 126334.
- Khezerlou, A., Tavassoli, M., Alizadeh Sani, M., Ehsani, A., & McClements, D. J. (2023). Smart Packaging for Food Spoilage Assessment Based on Hibiscus sabdariffa L. Anthocyanin-Loaded Chitosan Films. *Journal of Composites Science*, 7(10), 404.
- Kong, J., Ge, X., Sun, Y., Mao, M., Yu, H., Chu, R., & Wang, Y. (2023). Multi-functional pH-sensitive active and intelligent packaging based on highly cross-linked zein for the monitoring of pork freshness. *Food Chemistry*, 404, Article 134754.
- Lal, S., Kumar, V., & Arora, S. (2021). Eco-friendly synthesis of biodegradable and high strength ternary blend films of PVA/starch/pectin: Mechanical, thermal and biodegradation studies. *Polymers and Polymer Composites*, 29(9), 1505–1514.
- Li, T., Hu, W., Li, J., Zhang, X., Zhu, J., & Li, X. (2012). Coating effects of tea polyphenol and rosemary extract combined with chitosan on the storage quality of large yellow croaker (*Pseudosciaena crocea*). *Food Control*, 25(1), 101–106.
- Lin, X., Chen, S., Wang, R., Li, C., & Wang, L. (2023). Fabrication, characterization and biological properties of pectin and/or chitosan-based films incorporated with noni (*Morinda citrifolia*) fruit extract. *Food Hydrocolloids*, 134, Article 108025.
- Liu, J., Huang, J., Ying, Y., Hu, L., & Hu, Y. (2021). pH-sensitive and antibacterial films developed by incorporating anthocyanins extracted from purple potato or roselle into chitosan/polyvinyl alcohol/nano-ZnO matrix: Comparative study. *International Journal of Biological Macromolecules*, 178, 104–112.
- Liu, L., Wu, W., Zheng, L., Yu, J., Sun, P., & Shao, P. (2022). Intelligent packaging films incorporated with anthocyanins-loaded ovalbumin-carboxymethyl cellulose nanocomplexes for food freshness monitoring. *Food Chemistry*, 387, Article 132908.
- Martorana, M., Arcoraci, T., Rizza, L., Cristani, M., Bonina, F. P., Saija, A., Trombetta, D., & Tomaino, A. (2013). In vitro antioxidant and in vivo photoprotective effect of pistachio (*Pistacia vera* L., variety Bronte) seed and skin extracts. *FitoTerapia*, 85, 41–48.
- Mellinas, A. C., Jiménez, A., & Garrigós, M. C. (2020). Pectin-Based Films with Cocoa Bean Shell Waste Extract and ZnO/Zn-NPs with Enhanced Oxygen Barrier, Ultraviolet Screen and Photocatalytic Properties. *Foods*, 9(11), 1572.
- Mohammadian, E., Alizadeh-Sani, M., & Jafari, S. M. (2020). Smart monitoring of gas/temperature changes within food packaging based on natural colorants. *Comprehensive Reviews in Food Science and Food Safety*, 19(6), 2885–2931.
- Mohseni-Shahri, F. S., & Moeinpour, F. (2023). Development of a pH-sensing indicator for shrimp freshness monitoring: Curcumin and anthocyanin-loaded gelatin films. *Food Science & Nutrition*, 11(7), 3898–3910.
- Nadernejad, N., Ahmadi Moghadam, A., Hossyinfard, J., & Poorseyedi, S. (2013). Study of the rootstock and cultivar effect in PAL activity, production of phenolic and flavonoid compounds on flower, leaf and fruit in Pistachio (*Pistacia vera* L.). *Iranian Journal of Plant Biology*, 5(15), 95–110.
- Narayanan, G. P., Radhakrishnan, P., Baiju, P., & A. m. s. (2023). Fabrication Of Butterfly Pea Flower Anthocyanin-Incorporated Colorimetric Indicator Film Based On Gelatin/Pectin For Monitoring Fish Freshness. *Food Hydrocolloids for Health*, 4, Article 100159.
- Nobari, A., Marvizeh, M. M., Sadeghi, T., Rezaei-savadkouhi, N., & Mohammadi Nafchi, A. (2022). Flavonoid and Anthocyanin Pigments Characterization of Pistachio Nut (*Pistacia vera*) as a Function of Cultivar. *Journal of Nuts*, 13(4), 313–322.
- Norcino, L. B., Mendes, J. F., Natarelli, C. V. L., Manrich, A., Oliveira, J. E., & Mattoso, L. H. C. (2020). Pectin films loaded with copaiba oil nanoemulsions for potential use as bio-based active packaging. *Food Hydrocolloids*, 106, Article 105862.
- Qin, Y., Yun, D., Xu, F., Chen, D., Kan, J., & Liu, J. (2021). Smart packaging films based on starch/polyvinyl alcohol and Lycium ruthenicum anthocyanins-loaded nanocomplexes: Functionality, stability and application. *Food Hydrocolloids*, 119, Article 106850.
- Rawdkuen, S., Faseha, A., Benjakul, S., & Kaewprachu, P. (2020). Application of anthocyanin as a color indicator in gelatin films. *Food Bioscience*, 36, Article 100603.
- Sadi, A., & Ferfera-Harrar, H. (2023). Cross-linked CMC/Gelatin bio-nanocomposite films with organoclay, red cabbage anthocyanins and pistacia leaves extract as active intelligent food packaging: Colorimetric pH indication, antimicrobial/antioxidant properties, and shrimp spoilage tests. *International Journal of Biological Macromolecules*, 242, Article 124964.
- Sani, M. A., Dabbagh-Moghaddam, A., Jahed-Khaniki, G., Ehsani, A., Sharifan, A., Khezerlou, A., Tavassoli, M., & Maleki, M. (2023). Biopolymers-based multifunctional nanocomposite active packaging material loaded with zinc oxide nanoparticles, quercetin and natamycin; development and characterization. *Journal of Food Measurement and Characterization*, 17(3), 2488–2504.
- Siddiqui, J., Taheri, M., Alam, A. U., & Deen, M. J. (2022). Nanomaterials in smart packaging applications: A review. *Small*, 18(1), 2101171.
- Tavassoli, M., Alizadeh Sani, M., Khezerlou, A., Ehsani, A., Jahed-Khaniki, G., & McClements, D. J. (2022). Smart Biopolymer-Based Nanocomposite Materials Containing pH-Sensing Colorimetric Indicators for Food Freshness Monitoring. *Molecules*, 27(10), 3168.
- Tavassoli, M., Khezerlou, A., Moghaddam, T. N., Firoozy, S., Bakhshizadeh, M., Sani, M. A., Hashemi, M., Ehsani, A., & Lorenzo, J. M. (2023). Sumac (*Rhus coriaria* L.) anthocyanin loaded-pectin and chitosan nanofiber matrices for real-time monitoring of shrimp freshness. *International Journal of Biological Macromolecules*, 242, Article 125044.
- Wang, F., Xie, C., Tang, H., Hao, W., Wu, J., Sun, Y., Sun, J., Liu, Y., & Jiang, L. (2023). Development, characterization and application of intelligent/active packaging of chitosan/chitin nanofibers films containing eggplant anthocyanins. *Food Hydrocolloids*, 139, Article 108496.
- Ye, X., Liu, R., Qi, X., Wang, X., Wang, Y., Chen, Q., & Gao, X. (2022). Preparation of bioactive gelatin film using semi-refined pectin reclaimed from blueberry juice pomace: Creating an oxidation and light barrier for food packaging. *Food Hydrocolloids*, 129, Article 107673.
- Yong, H., & Liu, J. (2020). Recent advances in the preparation, physical and functional properties, and applications of anthocyanins-based active and intelligent packaging films. *Food Packaging and Shelf Life*, 26, Article 100550.
- Yun, D., He, Y., Zhu, H., Hui, Y., Li, C., Chen, D., & Liu, J. (2022). Smart packaging films based on locust bean gum, polyvinyl alcohol, the crude extract of *Loropetalum chinense* var. *rubrum* petals and its purified fractions. *International Journal of Biological Macromolecules*, 205, 141–153.
- Zarandona, I., Bengoechea, C., Álvarez-Castillo, E., de la Caba, K., Guerrero, A., & Guerrero, P. (2021). 3D Printed Chitosan-Pectin Hydrogels: From Rheological Characterization to Scaffold Development and Assessment. *Gels*, 7(4), 175.
- Zhang, W., Sani, M. A., Zhang, Z., McClements, D. J., & Jafari, S. M. (2023). High performance biopolymeric packaging films containing zinc oxide nanoparticles for fresh food preservation: A review. *International Journal of Biological Macromolecules*, 230, Article 123188.
- Zheng, Y., Li, X., Huang, Y., Li, H., Chen, L., & Liu, X. (2022). Two colorimetric films based on chitin whiskers and sodium alginate/gelatin incorporated with anthocyanins for monitoring food freshness. *Food Hydrocolloids*, 127, Article 107517.